

Dipole Modulation of Cosmic Microwave Background Temperature and Polarization.

Shamik Ghosh,^{1,*} Rahul Kothari,^{1,†} Pankaj Jain,^{1,‡} and Pranati K. Rath^{2,§}

¹*Dept. of Physics, Indian Institute of Technology,
Kanpur - 208016, India*

²*Institute of Physics,
Sachivalaya Marg, Bhubaneswar - 751005, Odisha, India*

(Dated: October 7, 2015)

Abstract

We propose a dipole modulation model for the Cosmic Microwave Background Radiation (CMBR) polarization field. We show that the model leads to correlations between l and $l + 1$ multipoles, exactly as in the case of temperature. We obtain results for the case of TE , EE and BB correlations. An anisotropic or inhomogeneous model of primordial power spectrum which leads to such correlations in temperature field also predicts similar correlations in CMBR polarization. We analyze the CMBR temperature and polarization data in order to extract the signal of these correlation between l and $l + 1$ multipoles. Our results for the case of temperature using the latest PLANCK data agree with those obtained by an earlier analysis. A detailed study of the correlation in the polarization data is not possible at present. Hence we restrict ourselves to a preliminary investigation in this case.

PACS numbers: 98.80.-k, 98.80.Es

* shamik@iitk.ac.in

† rahulko@iitk.ac.in

‡ pkjain@iitk.ac.in

§ pranati@iopb.res.in

I. INTRODUCTION

The Cosmic Microwave Background Radiation (CMB) shows a hemispherical power asymmetry, due to which the power in the two hemispheres is significantly different [1–8]. A dipole modulation of a statistically isotropic signal provides a useful parametrization of the observed power asymmetry. According to the model, the observed temperature fluctuation $\Delta\tilde{T}$ along a direction \hat{n} is expressed as [9–12],

$$\Delta\tilde{T}(\hat{n}) = \Delta T(\hat{n}) \left(1 + A\hat{\lambda}_1 \cdot \hat{n}\right), \quad (\text{I.1})$$

where $\Delta T(\hat{n})$ is a statistically isotropic field, A the dipole amplitude and $\hat{\lambda}_1$ the dipole direction. Throughout this paper we shall denote the observed fields, which are assumed to have some contribution due to dipole modulation, with a tilde and the corresponding fields in an isotropic model without a tilde. Choosing our axes such that $\hat{\lambda}_1$ is along \hat{z} , Eq. (I.1) can be written as

$$\Delta\tilde{T}(\hat{n}) = \Delta T(\hat{n}) (1 + A \cos \theta). \quad (\text{I.2})$$

As shown in [11, 13], the two point correlation of such a modulated temperature field would show correlations between l and $l + 1$.

If the observed signal of hemispherical anisotropy or equivalently dipole modulation is related to a physical effect, we expect a similar signal to be present in polarization fields too. Several studies have associated this effect with a primordial inhomogeneous or anisotropic model. Such models lead to a modification of the primordial power spectrum which culminates in depicting correlations between different multipoles similar to those predicted by Eq. I.1. In a recent paper it has been shown that such a primordial model also leads to correlations between l and $l + 1$ of the polarization fields. In this paper we propose a dipole modulation model for the CMBR polarization field, analogous to Eq. I.1. Such a model is useful to empirically characterize the observed hemispherical anisotropy that might be present in the polarization data, irrespective of the physical cause of its origin. We show that this model leads to correlations between the l and $l + 1$ multipoles for the polarization fields. We also determine the explicit form of these correlations.

We search for such correlations in the recently released Planck experiment data in both temperature and polarization signals and compare them with previous results and predictions. In the case of polarization a detailed study is not possible due to difficulty in handling and interpretation of the noise files. Hence in this case we restrict ourselves to a preliminary investigation.

II. TEST FOR DIPOLE MODULATION

The modulated temperature field is given by Eq. (I.2). This being a field on a sphere, can be expanded in spherical harmonics as

$$\Delta\tilde{T}(\hat{n}) = \sum_{l,m} \tilde{a}_{lm}^T Y_{lm}(\hat{n}) \quad (\text{II.1})$$

The two point correlation of the temperature field in multipole space can be written as

$$\langle \tilde{a}_{lm}^T \tilde{a}_{l'm'}^{T*} \rangle = \int d\Omega_{\hat{n}} d\Omega_{\hat{n}'} Y_{lm}^*(\hat{n}) Y_{l'm'}(\hat{n}') \langle \Delta\tilde{T}(\hat{n}) \Delta\tilde{T}(\hat{n}') \rangle \quad (\text{II.2})$$

As shown in [13], using Eq. (I.2) we obtain

$$\langle \tilde{a}_{lm}^T \tilde{a}_{l'm'}^{T*} \rangle = C_l^T \delta_{ll'} \delta_{mm'} + A (C_{l'}^T + C_l^T) \xi_{lm;l'm'}^0 \quad (\text{II.3})$$

where

$$\xi_{lm;l'm'}^0 = \delta_{mm'} \left[\sqrt{\frac{(l+m+1)(l-m+1)}{(2l+3)(2l+1)}} \delta_{l',l+1} + \sqrt{\frac{(l+m)(l-m)}{(2l+1)(2l-1)}} \delta_{l',l-1} \right] \quad (\text{II.4})$$

In Eq. (II.3), the first term on RHS corresponds to the isotropic part of the correlation $\langle \tilde{a}_{lm}^T \tilde{a}_{l'm'}^{T*} \rangle_{\text{iso}}$ and the second term is the contribution of the modulation, $\langle \tilde{a}_{lm}^T \tilde{a}_{l'm'}^{T*} \rangle_{\text{mod}}$. As we shall see the multipole power C_l^T does not get any contribution from the modulation term. This is found to be true also for the power in the polarization fields, to be discussed later. Hence we do not denote it with a tilde. We follow [13] and seek correlations between l and $l+1$ multipoles, which can be expressed as,

$$\langle \tilde{a}_{lm}^T \tilde{a}_{l+1m}^{T*} \rangle = A [C_{l+1}^T + C_l^T] \sqrt{\frac{(l+m+1)(l-m+1)}{(2l+3)(2l+1)}}. \quad (\text{II.5})$$

Theoretical models used to explain the dipole modulation of the temperature field predict a similar correlation between l and $l+1$ multipoles in the CMB E-mode polarization field [14, 15] in the same direction. These predictions may be tested in future by determining these correlations in the CMB polarization field.

A detailed discussion of CMB polarization is contained in [16, 17] and here we use the notation of [16]. The CMB polarization field is characterized by two Stokes parameters \tilde{Q} and \tilde{U} , while the temperature fluctuation field corresponds to Stokes' parameter \tilde{I} . Here \tilde{Q} and \tilde{U} denote the dipole modulated polarization fields. Under a rotation by an angle ψ , the temperature field transforms as a scalar, while combinations of \tilde{Q} and \tilde{U} behave as spin ± 2 fields on a sphere, viz.

$$(\tilde{Q} \pm i\tilde{U})'(\hat{n}) = e^{\mp 2i\psi} (\tilde{Q} \pm i\tilde{U})(\hat{n}), \quad (\text{II.6})$$

and can be expanded in spin ± 2 harmonics as

$$(\tilde{Q} \pm i\tilde{U})(\hat{n}) = \sum_{lm} \tilde{a}_{\pm 2, lm} Y_{lm}(\hat{n}). \quad (\text{II.7})$$

Using the spin raising and lowering operators $\tilde{\partial}$ and $\tilde{\partial}^\dagger$, spin 0 objects can be constructed from \tilde{Q} and \tilde{U} fields [18]. Using $\tilde{\partial}$ and $\tilde{\partial}^\dagger$ suitably on Eq. (II.7) we get

$$\tilde{\partial}^2(\tilde{Q} + i\tilde{U})(\hat{n}) = \sum_{lm} \sqrt{\frac{(l+2)!}{(l-2)!}} \tilde{a}_{2, lm} Y_{lm}(\hat{n}) \quad (\text{II.8})$$

$$\tilde{\partial}^2(\tilde{Q} - i\tilde{U})(\hat{n}) = \sum_{lm} \sqrt{\frac{(l+2)!}{(l-2)!}} \tilde{a}_{-2, lm} Y_{lm}(\hat{n}). \quad (\text{II.9})$$

Finally the standard E and B mode polarization field can be expressed as,

$$\tilde{E}(\hat{n}) = -\frac{1}{2} [\tilde{\partial}^2(\tilde{Q} + i\tilde{U}) + \tilde{\partial}^2(\tilde{Q} - i\tilde{U})] = \sum_{lm} \sqrt{\frac{(l+2)!}{(l-2)!}} \tilde{a}_{lm}^E Y_{lm}(\hat{n}) \quad (\text{II.10})$$

$$\tilde{B}(\hat{n}) = \frac{i}{2} [\tilde{\partial}^2(\tilde{Q} + i\tilde{U}) - \tilde{\partial}^2(\tilde{Q} - i\tilde{U})] = \sum_{lm} \sqrt{\frac{(l+2)!}{(l-2)!}} \tilde{a}_{lm}^B Y_{lm}(\hat{n}). \quad (\text{II.11})$$

The coefficients \tilde{a}_{lm}^E and \tilde{a}_{lm}^B are defined as linear combinations of $\tilde{a}_{\pm 2, lm}$ as:

$$\tilde{a}_{lm}^E = -\frac{1}{2} (\tilde{a}_{2, lm} + \tilde{a}_{-2, lm}) \quad (\text{II.12})$$

$$\tilde{a}_{lm}^B = \frac{i}{2} (\tilde{a}_{2, lm} - \tilde{a}_{-2, lm}) \quad (\text{II.13})$$

The \tilde{a}_{lm}^E s define the E-mode polarization in multipole space and are unchanged under parity transformation in contrast to \tilde{a}_{lm}^B s which do change sign under such a transformation. The scalar fields defined in Eqs. (II.10) and (II.11) are the real space constructs of the E-mode and B-mode polarizations representing the irrotational and curl components of the CMB polarizations respectively. In this work we are interested in the E-mode field. We define the auto correlation of the E field and cross correlation of the E and T fields as

$$C_l^{EE} = \frac{1}{2l+1} \sum_m \langle \tilde{a}_{lm}^E \tilde{a}_{lm}^{E*} \rangle \quad (\text{II.14})$$

$$C_l^{TE} = \frac{1}{2l+1} \sum_m \langle \tilde{a}_{lm}^E \tilde{a}_{lm}^{T*} \rangle \quad (\text{II.15})$$

In order to study the l and $l+1$ correlations we construct

$$C_{l, l+1}^{XX} = \frac{l(l+1)}{(2l+1)} \sum_{m=-l}^{m=l+1} \langle \tilde{a}_{lm}^X \tilde{a}_{l+1, m}^{X*} \rangle, \quad (\text{II.16})$$

and define our statistics as

$$S_H^{XX} = \sum_{l_{\min}}^{l_{\max}} C_{l,l+1}^{XX}. \quad (\text{II.17})$$

Here X can be either T or E giving us TT , EE , TE and ET correlations. We search the direction for which the statistic S_H^{XX} maximizes in each of the maps. We also define a quantity R as the ratio of the anisotropic part to isotropic part, i.e.,

$$R = \frac{\sum_{l_{\min}}^{l_{\max}} C_{l,l+1}^{XX}}{\sum_{l_{\min}}^{l_{\max}} l(l+1)C_l^{XX}} \quad (\text{II.18})$$

This may be seen as a measure of the fraction of the anisotropic effect to the isotropic power.

III. DIPOLE MODULATION IN POLARIZATION

The dipole modulated polarization fields are denoted by $\tilde{Q}(\hat{n})$ and $\tilde{U}(\hat{n})$ where $\hat{n} \equiv (\theta, \phi)$. We also define

$$\tilde{\alpha}_{\pm}(\hat{n}) = \tilde{Q}(\hat{n}) \pm i\tilde{U}(\hat{n}), \quad (\text{III.1})$$

$\alpha_{\pm}(\hat{n}) = Q(\hat{n}) \pm iU(\hat{n})$ where Q and U are the standard unmodulated fields in an isotropic model, $\tilde{\alpha}_{-} = \tilde{\alpha}_{+}^{*}$ and $\alpha_{-} = \alpha_{+}^{*}$. The preferred direction $\hat{\lambda}$ is taken to be the same for both \tilde{Q} and \tilde{U} as well as the temperature field [15]. In analogy with temperature, we propose the following model for dipole modulation of polarization:

$$\begin{aligned} \tilde{\alpha}_{+}(\hat{n}) &= \alpha_{+}(\hat{n}) \left(1 + A_P \hat{\lambda} \cdot \hat{n} \right), \\ \tilde{\alpha}_{-}(\hat{n}) &= \alpha_{-}(\hat{n}) \left(1 + A_P^{*} \hat{\lambda} \cdot \hat{n} \right). \end{aligned} \quad (\text{III.2})$$

Here $A_P = A_1 + iA_2$ is a complex parameter. We choose our coordinates such that $\hat{\lambda} = \hat{z}$ and hence $\hat{\lambda} \cdot \hat{n} = \cos \theta$. In terms of the Stokes' parameters, we obtain

$$\begin{aligned} \tilde{Q} &= Q(1 + A_1 \cos \theta) - UA_2 \cos \theta \\ \tilde{U} &= QA_2 \cos \theta + U(1 + A_1 \cos \theta) \end{aligned} \quad (\text{III.3})$$

Using Eqs. II.7 and II.13 for the modulated polarization fields, we obtain

$$\tilde{\alpha}_{\pm} = - \sum_{lm} (\tilde{a}_{lm}^E \pm i\tilde{a}_{lm}^B) {}_{\pm 2}Y_{lm}, \quad (\text{III.4})$$

where $\tilde{a}_{E,lm}$ and $\tilde{a}_{B,lm}$ denote the harmonic coefficients of the modulated fields. Inverting the above equation we obtain

$$-(\tilde{a}_{lm}^E \pm i\tilde{a}_{lm}^B) = \int \tilde{\alpha}_{\pm}(\hat{n}) {}_{\pm 2}Y_{lm}^{*}(\hat{n}) d\Omega. \quad (\text{III.5})$$

This leads to

$$\tilde{a}_{lm}^E = -\frac{1}{2} \int [\alpha_+(\hat{n})(1 + A_P \cos \theta) {}_2Y_{lm}^*(\hat{n}) + \alpha_-(\hat{n})(1 + A_P^* \cos \theta) {}_2Y_{lm}^*(\hat{n})] d\Omega, \quad (\text{III.6})$$

where we have used Eq. (III.2). We also obtain a similar equation for $\tilde{a}_{B,lm}$.

A. Correlations of the Dipole Modulated Polarization Field

The two point correlations of the dipole modulated E field harmonic coefficients can be expressed as,

$$\langle \tilde{a}_{lm}^E \tilde{a}_{l'm'}^{E*} \rangle = \frac{1}{4} (I_1 + I_2 + I_3 + I_4) \quad (\text{III.7})$$

where

$$\begin{aligned} I_1 &= \iint d\Omega d\Omega' \langle \alpha_+(\hat{n}) \alpha_-(\hat{n}') \rangle (1 + A_P \cos \theta) (1 + A_P^* \cos \theta') {}_2Y_{lm}^*(\hat{n}) {}_2Y_{l'm'}(\hat{n}'), \\ I_2 &= \iint d\Omega d\Omega' \langle \alpha_+(\hat{n}) \alpha_+(\hat{n}') \rangle (1 + A_P \cos \theta) (1 + A_P \cos \theta') {}_2Y_{lm}^*(\hat{n}) {}_2Y_{l'm'}(\hat{n}'), \\ I_3 &= \iint d\Omega d\Omega' \langle \alpha_-(\hat{n}) \alpha_-(\hat{n}') \rangle (1 + A_P^* \cos \theta) (1 + A_P^* \cos \theta') {}_2Y_{lm}^*(\hat{n}) {}_2Y_{l'm'}(\hat{n}'), \\ I_4 &= \iint d\Omega d\Omega' \langle \alpha_-(\hat{n}) \alpha_+(\hat{n}') \rangle (1 + A_P^* \cos \theta) (1 + A_P \cos \theta') {}_2Y_{lm}^*(\hat{n}) {}_2Y_{l'm'}(\hat{n}'). \end{aligned}$$

The two point correlations appearing on the right hand side of these equations can be written as:

$$\begin{aligned} \langle \alpha_+(\hat{n}) \alpha_-(\hat{n}') \rangle &= \sum_{l''m''} (C_{l''}^{EE} + C_{l''}^{BB}) {}_2Y_{l''m''}(\hat{n}) {}_2Y_{l''m''}^*(\hat{n}'), \\ \langle \alpha_+(\hat{n}) \alpha_+(\hat{n}') \rangle &= \sum_{l''m''} (C_{l''}^{EE} - C_{l''}^{BB}) (-1)^{m''} {}_2Y_{l''m''}(\hat{n}) {}_2Y_{l''(-m'')}^*(\hat{n}'), \\ \langle \alpha_-(\hat{n}) \alpha_-(\hat{n}') \rangle &= \sum_{l''m''} (C_{l''}^{EE} - C_{l''}^{BB}) (-1)^{m''} {}_2Y_{l''m''}^*(\hat{n}) {}_2Y_{l''(-m'')}(\hat{n}'), \\ \langle \alpha_-(\hat{n}) \alpha_+(\hat{n}') \rangle &= \sum_{l''m''} (C_{l''}^{EE} + C_{l''}^{BB}) {}_2Y_{l''m''}^*(\hat{n}) {}_2Y_{l''(-m'')}(\hat{n}'). \end{aligned}$$

where we have used, $\langle a_{lm}^E a_{l'm'}^{E*} \rangle = C_l^E \delta_{ll'} \delta_{mm'}$, $\langle a_{lm}^B a_{B,l'm'}^{B*} \rangle = C_l^B \delta_{ll'} \delta_{mm'}$, $\langle a_{lm}^E a_{l'm'}^{B*} \rangle = 0$ and ${}_2Y_{lm}^* = (-1)^m {}_2Y_{l(-m)}$. Here C_l^E and C_l^B represent the isotropic power spectrum corresponding to E or B modes respectively. As we shall see the anisotropic model does not contribute to the power spectrum. Hence these also represent the power of the tilde fields.

Substituting the resulting expressions of I_i in Eq. III.7, we obtain

$$\langle \tilde{a}_{lm}^E \tilde{a}_{l'm'}^{E*} \rangle = C_l^{EE} \delta_{ll'} \delta_{mm'} + \frac{1}{4} (M_1 + M_2 + M_3 + M_4) \quad (\text{III.8})$$

where M_i represent the corrections due to dipole modulation and are given by,

$$\begin{aligned}
M_1 &= \sum_{l''m''} (C_{l''}^{EE} + C_{l''}^{BB}) \iint d\Omega d\Omega' (A_P \cos \theta + A_P^* \cos \theta') {}_2Y_{l''m''}(\hat{n}) {}_2Y_{l''m''}^*(\hat{n}') {}_2Y_{lm}^*(\hat{n}) {}_2Y_{l'm'}(\hat{n}'), \\
M_2 &= \sum_{l''m''} (C_{l''}^{EE} - C_{l''}^{BB}) (-1)^{m''+m'} \iint d\Omega d\Omega' (A_P \cos \theta' + A_P \cos \theta) {}_2Y_{l''m''}(\hat{n}) {}_2Y_{l''(-m'')}(\hat{n}') \\
&\quad \times {}_2Y_{lm}^*(\hat{n}) {}_2Y_{l'(-m')}^*(\hat{n}'), \\
M_3 &= \sum_{l''m''} (C_{l''}^{EE} - C_{l''}^{BB}) (-1)^{m''+m} \iint d\Omega d\Omega' (A_P^* \cos \theta + A_P^* \cos \theta') {}_2Y_{l''m''}^*(\hat{n}') {}_2Y_{l''(-m'')}(\hat{n}) \\
&\quad \times {}_2Y_{l(-m)}(\hat{n}) {}_2Y_{l'm'}(\hat{n}'), \\
M_4 &= \sum_{l''m''} (C_{l''}^{EE} + C_{l''}^{BB}) (-1)^{m'+m} \iint d\Omega d\Omega' (A_P^* \cos \theta + A_P \cos \theta') {}_2Y_{l''(-m'')}^*(\hat{n}) {}_2Y_{l''(-m'')}(\hat{n}') \\
&\quad \times {}_2Y_{l(-m)}(\hat{n}) {}_2Y_{l'(-m')}^*(\hat{n}').
\end{aligned}$$

where we have assumed that the modulation parameters A_1 and A_2 are small and dropped higher order terms. We can evaluate these integrals by using

$$\int_0^{2\pi} \int_0^\pi {}_2Y_{lm}(\hat{n}) {}_2Y_{l'm'}^*(\hat{n}) d\Omega = \delta_{ll'} \delta_{mm'}. \quad (\text{III.9})$$

Furthermore we define

$$\mathbb{I}(l, m, l', m') = \int_0^{2\pi} \int_0^\pi {}_2Y_{lm}(\hat{n}) {}_2Y_{l'm'}^*(\hat{n}) \cos \theta d\Omega = \delta_{m,m'} \mathbb{K}(l, l', m), \quad (\text{III.10})$$

This integral can be expressed in terms of the Wigner 3-j symbols by using

$$Y_{10}(\hat{n}) = \sqrt{\frac{3}{4\pi}} \cos \theta. \quad (\text{III.11})$$

We obtain

$$\mathbb{I}(l, m, l', m') = (-1)^{m'} \sqrt{(2l+1)(2l'+1)} \begin{pmatrix} l' & l & 1 \\ 2 & -2 & 0 \end{pmatrix} \begin{pmatrix} l' & l & 1 \\ -m' & m & 0 \end{pmatrix} \quad (\text{III.12})$$

The Wigner 3-j symbol obeys the condition,

$$\begin{pmatrix} l_1 & l_2 & l_3 \\ m_1 & m_2 & m_3 \end{pmatrix} = 0 \quad \text{if } |l_1 - l_2| > l_3 \quad (\text{III.13})$$

Using this we find that

$$\mathbb{K}(l, l', m) = 0 \quad \text{if } l' > l+1 \text{ and } l' < l-1 \quad (\text{III.14})$$

For the remaining cases, $l = l'$ and $l' = l \pm 1$, it can be expressed as,

$$\mathbb{K}(l, l', m) = (-1)^{l+l'} H(l, l', m) \mathbb{U}(l, l', m), \quad (\text{III.15})$$

where

$$H(l, l', m) = -2 \sqrt{\frac{(2l+1)(2l'+1)(l-m)!(l+m)!(l'-m)!(l'+m)!}{(l+2)!(l-2)!(l'+2)!(l'-2)!}}.$$

$$\mathbb{U}(l, l', m) = \frac{(2l)!(l'+2)!(l'-2)!\delta_{l+1,l'}}{(2l+3)!(l-m)!(l+m)!} + \frac{2m(2l)!(l+2)!(l-2)!\delta_{l,l'}}{l(l+m)!(l-m)!(2l+2)!} + \frac{(2l')!(l-2)!(l+2)!\delta_{l-1,l'}}{(l'+m)!(l'-m)!(2l+1)!}.$$

The function $\mathbb{K}(l, l', m)$ is explicitly evaluated in the next subsection. We can now write the integrals M_i as

$$\begin{aligned} M_1 &= (-1)^{l+l'} \delta_{mm'} H(l', l, m) \mathbb{U}(l', l, m) [A_P (C_{l'}^{EE} + C_{l'}^{BB}) + A_P^* (C_l^{EE} + C_l^{BB})], \\ M_2 &= (-1)^{l+l'} \delta_{mm'} A_P [H(l, l', -m) \mathbb{U}(l, l', -m) (C_l^{EE} - C_l^{BB}) + H(l', l, m) \mathbb{U}(l', l, m) (C_{l'}^{EE} - C_{l'}^{BB})], \\ M_3 &= (-1)^{l+l'} \delta_{mm'} A_P^* [H(l, l', -m) \mathbb{U}(l, l', -m) (C_{l'}^{EE} - C_{l'}^{BB}) + H(l', l, m) \mathbb{U}(l', l, m) (C_l^{EE} - C_l^{BB})], \\ M_4 &= (-1)^{l+l'} \delta_{mm'} H(l, l', -m) \mathbb{U}(l, l', -m) [A_P^* (C_{l'}^{EE} + C_{l'}^{BB}) + A_P (C_l^{EE} + C_l^{BB})]. \end{aligned}$$

where we have used

$$\mathbb{U}(l, l', m) = \mathbb{U}(l', l, m)$$

and

$$H(l, l', m) = H(l', l, m) = H(l, l', -m) = H(l', l, -m).$$

This finally leads to

$$\langle \tilde{a}_{lm}^E \tilde{a}_{l'm'}^{E*} \rangle = C_l^{EE} \delta_{ll'} \delta_{mm'} + \delta_{mm'} \frac{1}{2} [\mathbb{K}(l, l', m) (A_P C_{l'}^{EE} + A_P^* C_l^{EE}) + \mathbb{K}(l, l', -m) (A_P^* C_{l'}^{EE} + A_P C_l^{EE})].$$

The first term on the right hand side of this equation is the standard contribution due to an isotropic field. The second term arises due to dipole modulation. In this term only contributions linear in the dipole parameters A_1 and A_2 have been kept. We see that the modulation model, Eq. III.2, leads to correlations between multipoles l and $l+1$ besides also leading to additional contributions proportional to $\delta_{mm'} \delta_{ll'}$. However the latter contributions cancel out after summing over m and can be ignored. Hence after summing over m the dipole modulation term leads to correlations only between l and $l+1$. We also notice that the terms proportional to $\delta_{l+1,l'}$ and $\delta_{l-1,l'}$ in Eq. III.15 are symmetric under the interchange $m \leftrightarrow -m$. Hence we deduce that $\mathbb{K}(l, l', m) = \mathbb{K}(l, l', -m)$. Using this we obtain

$$\langle \tilde{a}_{lm}^E \tilde{a}_{l'm'}^{E*} \rangle = C_l^{EE} \delta_{ll'} \delta_{mm'} + \delta_{mm'} A_1 \mathbb{K}(l, l', m) (C_{l'}^{EE} + C_l^{EE}). \quad (\text{III.16})$$

where we have ignored the contributions proportional to $\delta_{l,l'}$ since they cancel out after summing over m . Similarly for the B mode polarization, we obtain

$$\langle \tilde{a}_{lm}^B \tilde{a}_{l'm'}^{B*} \rangle = C_l^{BB} \delta_{ll'} \delta_{mm'} + \delta_{mm'} A_1 \mathbb{K}(l, l', m) (C_{l'}^{BB} + C_l^{BB}). \quad (\text{III.17})$$

The dipole modulation model, Eq. III.2, is very useful for characterizing a signal of anisotropic power that might exist in the polarization data. It allows an empirical parametrization of such a signal. Furthermore it can be used to perform simulations which are required for a statistical study of the anisotropy. We explicitly demonstrate this in the present paper. We also point out that an alternate model in which we may directly introduce a dipole modulation in the E mode polarization simply does not work.

The correlations of the E and B mode multipoles, Eqs. III.16 and III.17 depend only on the parameter A_1 and are independent of A_2 . Hence we can directly extract A_1 by studying the E mode correlations.

A similar calculation for the TE mode correlations leads to the following result

$$\langle \tilde{a}_{lm}^{T*} \tilde{a}_{l'm'}^E \rangle = C_l^{TE} \delta_{ll'} \delta_{mm'} + AC_{l'}^{TE} \xi_{lm;l'm'}^0 + \frac{1}{2} A_P C_l^{TE} \delta_{mm'} \mathbb{K}(l, l', m) + \frac{1}{2} A_P^* C_l^{TE} \delta_{mm'} \mathbb{K}(l, l', -m) \quad (\text{III.18})$$

In this case also, after summing over m , the $\delta_{ll'}$ term in $\mathbb{K}(l, l', m)$ and $\mathbb{K}(l, l', -m)$ drops out. Hence it can be ignored and the remaining terms are symmetric under $m \leftrightarrow -m$. Therefore we can express this result as

$$\langle \tilde{a}_{lm}^{T*} \tilde{a}_{l'm'}^E \rangle = C_l^{TE} \delta_{ll'} \delta_{mm'} + AC_{l'}^{TE} \xi_{lm;l'm'}^0 + A_1 C_l^{TE} \delta_{mm'} \mathbb{K}(l, l', m) \quad (\text{III.19})$$

B. Calculation of the Polarization Correlations

We next explicitly evaluate the integral in Eq. (III.10). The spin 2 harmonics [19] can be expressed as

$$\begin{aligned} {}_2Y_{lm} &= (-1)^m e^{im\phi} \sqrt{\frac{(2l+1)(l-m)!(l+m)!}{4\pi(l+2)!(l-2)!}} \\ &\times \sum_{r=0}^{l-2} (-1)^{l-r} \binom{l-2}{r} \binom{l+2}{r+2-m} \left(\sin \frac{\theta}{2}\right)^{2l-2r-2+m} \left(\cos \frac{\theta}{2}\right)^{2r+2-m}. \end{aligned} \quad (\text{III.20})$$

The ϕ integration in Eq. (III.10) leads to the factor $2\pi\delta_{mm'}$. The θ integral is evaluated by using the identity

$$\int_0^\pi d\theta \cos \theta \sin \theta \sin^m \left(\frac{\theta}{2}\right) \cos^n \left(\frac{\theta}{2}\right) = 2 \frac{\Gamma(\frac{m+2}{2}) \Gamma(\frac{n+4}{2})}{\Gamma(\frac{m+n+6}{2})} - 2 \frac{\Gamma(\frac{m+4}{2}) \Gamma(\frac{n+2}{2})}{\Gamma(\frac{m+n+6}{2})}. \quad (\text{III.21})$$

which can be derived by using [20]

$$\int_0^{\pi/2} \sin^m \theta \cos^n \theta d\theta = \frac{\Gamma\left(\frac{m+1}{2}\right) \Gamma\left(\frac{n+1}{2}\right)}{2\Gamma\left(\frac{m+n+2}{2}\right)}.$$

The function $\mathbb{I}(l, m, l', m')$ defined in Eq. III.10 can now be expressed as

$$\mathbb{I}(l, m, l', m') = (-1)^{l+l'} \delta_{mm'} H(l, l', m) \mathbb{U}(l, l', m), \quad (\text{III.22})$$

where

$$\mathbb{U}(l, l', m) = -\frac{(l-2)!(l+2)!(l'+2)!(l'-2)!}{2(l'+l+2)!} \mathbb{S}(l, l', m), \quad (\text{III.23})$$

$$\mathbb{S}(l, l', m) = \sum_{r=0}^{l-2} \sum_{t=0}^{l'-2} \mathcal{F}(l, l', r, t, m) \quad (\text{III.24})$$

and

$$\mathcal{F}(l, l', r, t, m) = \frac{(-1)^{r+t} (l+l'-r-t+m-2)! (r+t-m+2)! (2r+2t-2m+4-l-l')}{r! t! (l-2-r)! (l'-2-t)! (r+2-m)! (t+2-m)! (l-r+m)! (l'-t+m)!}. \quad (\text{III.25})$$

We next show that for $l' = l$,

$$\mathbb{S}(l, l', m) = \frac{-4m(2l)!}{l(l+m)!(l-m)!(l+2)!(l-2)!}. \quad (\text{III.26})$$

Proof: For $l = l'$,

$$\mathbb{S}(l, l', m) = \sum_{r=0}^{l-2} \frac{(-1)^r \binom{l+2}{l-r+m} \binom{l-2}{r}}{(l-2)!(l+2)!(l-2)!} \mathbb{P} \quad (\text{III.27})$$

where

$$\mathbb{P} = \sum_{t=0}^{l-2} (-1)^t \binom{l-2}{t} (2r+2t-2m+4-2l) \times \prod_{s=1}^{l-2-r} (l-t+m+s) \prod_{v=1}^r (t-m+2+v). \quad (\text{III.28})$$

We next express the two products as,

$$\prod_{s=1}^{l-2-r} (l-t+m+s) \prod_{v=1}^r (t-m+2+v) = (-1)^{l-2-r} \left[t^{l-2} + a_1 t^{l-3} + a_2 t^{l-4} + \dots + a_{l-2} \right],$$

where $a_i \in \mathbb{Z}$. Eq. III.28 now becomes,

$$\mathbb{P} = (-1)^{l-2-r} \sum_{t=0}^{l-2} (-1)^t \binom{l-2}{t} (2r+2t-2m+4-2l) \left[t^{l-2} + a_1 t^{l-3} + a_2 t^{l-4} + \dots + a_{l-2} \right].$$

By using Eq. VII.3 we find that only two terms, i.e. those proportional to t^{l-1} and t^{l-2} , contribute.

Thus we obtain

$$\mathbb{P} = (-1)^{l-2-r} \sum_{t=0}^{l-2} (-1)^t \binom{l-2}{t} \left[(2r-2m+4-2l+2a_1) t^{l-2} + 2t^{l-1} \right]. \quad (\text{III.29})$$

The constant a_1 can be determined by using the result that if

$$\prod_{i=1}^n (x + \alpha_i) = x^n + x^{n-1}a_1 + \dots a_n,$$

then $a_1 = \sum_{i=1}^n \alpha_i$. Thus we obtain

$$a_1 = \sum_{s=1}^{l-2-r} (-l-m-s) + \sum_{v=1}^r (-m+2+v) = \frac{1}{2} [-3l^2 + 7l - 2ml + 4m - 2 + 2r(2l+1)].$$

Using Eq. VII.3 we can express Eq. III.29 as,

$$\mathbb{P} = (-1)^{-r} (l-2)! [-2l^2 + 2l - 2ml + 2m + 4r(l+1)].$$

Substituting in Eq. III.27 we obtain

$$\mathbb{S}(l, l', m) = \sum_{r=0}^{l-2} \binom{l+2}{l-r+m} \binom{l-2}{r} \frac{[-2l^2 + 2l - 2ml + 2m + 4r(l+1)]}{(l+2)!(l-2)!}.$$

This sum can be divided into two parts

$$\frac{(-2l^2 + 2l - 2ml + 2m)}{(l+2)!(l-2)!} \sum_{r=0}^{l-2} \binom{l+2}{l-r+m} \binom{l-2}{r} + \frac{4(l+1)}{(l+2)!(l-2)!} \sum_{r=0}^{l-2} r \binom{l+2}{l-r+m} \binom{l-2}{r},$$

In the second sum $r=0$ does not contribute. Hence after some simplifications, it can be re-expressed as,

$$\frac{4(l-2)(l+1)}{(l+2)!(l-2)!} \sum_{t=0}^{l-3} \binom{l+2}{l-t-1+m} \binom{l-3}{t}.$$

We can evaluate both of these sums by using the Vandermonde Convolution property of binomial coefficients [21] which can be stated as,

$$\sum_{k=0}^m \binom{m}{k} \binom{p}{n-k} = \binom{m+p}{n}, \quad m+p \geq n \text{ \& } m, n, p \geq 0.$$

We finally obtain

$$\begin{aligned} \mathbb{S}(l, l', m) &= \frac{(-2l^2 + 2l - 2ml + 2m + 4)(2l)!}{(l+m)!(l-m)!(l+2)!(l-2)!} + \frac{4(l+1)(l-2)(2l-1)!}{(l+2)!(l-2)!(l-m)!(l-1+m)!} \\ &= \frac{-4m(2l)!}{l(l+m)!(l-m)!(l+2)!(l-2)!}, \end{aligned} \quad (\text{III.30})$$

which is the desired result and leads to $\mathbb{U}(l, l', m)$ given in Eq. III.15 for the case $l = l'$.

We next show that

$$\mathbb{S}(l, l', m) = - \begin{cases} \frac{2(2l)!}{(l+m)!(l-m)!(l+2)!(l-2)!} & l' = l+1 \\ \frac{2(2l')!}{(l'+m)!(l'-m)!(l'+2)!(l'-2)!} & l' = l-1 \end{cases} \quad (\text{III.31})$$

Proof: We first consider the case $l' = l + 1$. We can write Eq. (III.25) as

$$\begin{aligned} \mathcal{F}(l, l', r, t, m) &= (-1)^{r+t} \binom{l+2}{l-r+m} \binom{l'-2}{t} \frac{(2r+2t-2m+4-l-l')}{(l'-2)!(l+2)!} \\ &\times \left[\frac{(l+l'-r-t+m-2)!}{(l-r-2)!(l'-t+m)!} \right] \left[\frac{(r+t-m+2)!}{r!(t+2-m)!} \right]. \end{aligned} \quad (\text{III.32})$$

After simplification of the terms in the two square brackets, this becomes

$$\frac{(-1)^{r+t} \binom{l+2}{l-r+m} \binom{l-2}{r} \binom{l'-2}{t}}{(l'-2)!(l+2)!(l-2)!} \left[(2r+2t-2m+4-l-l') \prod_{s=1}^{l-2-r} (l'-t+m+s) \prod_{v=1}^r (t-m+2+v) \right].$$

We can write the term in the square brackets above as $a_0 t^{l-1} + a_1 t^{l-2} \dots a_{l-1}$, where $a_i \in \mathbb{Z}$. Keeping r fixed, the sum over t in Eq. III.24 yields,

$$\sum_{t=0}^{l'-2} \mathcal{F}(l, l', r, t, m) = \sum_{t=0}^{l'-2} (-1)^t \binom{l'-2}{t} [a_0 t^{l-1} + a_1 t^{l-2} + \dots + a_{l-1}]. \quad (\text{III.33})$$

By using Eq. III.32 on the left hand side and by comparing both sides, we find that a_0 is equal to $2(-1)^{l-2-r}$. Using the second case of Eq. VII.3 we obtain

$$\sum_{t=0}^{l'-2} \mathcal{F}(l, l', r, t, m) = -2(-1)^{-r} (l-1)! = -2(-1)^r (l-1)!$$

Finally the sum over r , after simplification, yields

$$\mathbb{S}(l, l', m) = -\frac{-2}{(l+2)!(l-2)!} \left[\sum_{r=0}^{l-2} \binom{l+2}{l-r+m} \binom{l-2}{r} \right] = \frac{-2(2l)!}{(l+2)!(l-2)!(l+m)!(l-m)!},$$

where we have again used the Vandermonde Convolution property. A similar analysis for the case $l' = l - 1$ yields

$$\mathbb{S}(l, l', m) = -\frac{-2(2l')!}{(l'+2)!(l'-2)!(l'+m)!(l'-m)!}.$$

These lead to the result for $\mathbb{U}(l, l', m)$ given in Eq. III.15 for the cases $l' = l \pm 1$

IV. DATA ANALYSIS

For the case of temperature data, we perform a detailed analysis of the signal. This allows us to obtain updated results for the statistic S_H^{TT} with the 2015 Planck data. We studied this statistic in the multipole ranges $2 \leq l \leq 64$, $30 \leq l \leq 64$ and $30 \leq l \leq 100$ in the Planck 2015 CMB intensity maps. The dipole modulation signal in the CMB temperature map was observed in the multipole range $2 - 64$ [22].

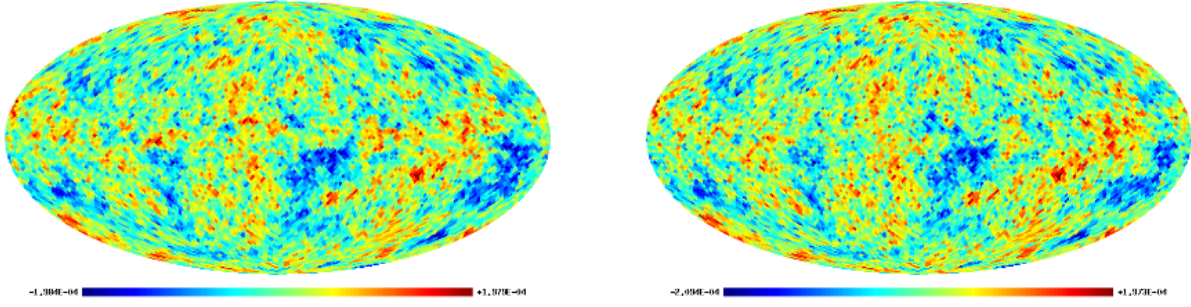


FIG. 1. Left: SMICA inpainted temperature map. Right: SMICA temperature map with the masked portions filled by isotropic randomly generated data. Both maps are for $N_{\text{side}} = 32$ and the temperature is given in units of K.

For the case of CMB polarization a detailed analysis is not possible at this stage since the data for low l is unreliable. Furthermore we are unable to properly simulate the noise corresponding to PLANCK detectors. Hence, even for large l , it is not possible for us to obtain a reliable estimate of the errors and the significance of the signal. For this reason we confine ourselves to a preliminary analysis of the polarization signal. However it may still serve a useful purpose in revealing the preferred direction indicated by data. We searched for modulation signal in the multipole ranges $40 - 100$, $40 - 125$, $50 - 100$, $50 - 125$, $50 - 150$ and $50 - 200$. The lower limit of $l = 40$ was chosen since the data for lower l is so far poorly understood.

A. Planck 2015 temperature data analysis

We have performed our analysis on both Commander and SMICA IQU maps. For SMICA maps, we have performed the analysis after masking the maps and then inpainting the masked maps using the MRS package of iSAP software or alternatively masking and then filling the masked portion of the map with isotropic data generated using the CAMB simulation package with Planck 2015 parameter set. The data analysis was performed with HEALPix software [23].

The analysis of the Commander and SMICA inpainted maps was performed identically. The maps were downgraded, without any smoothing to either $N_{\text{side}} = 32$, for multipole ranges $2 - 64$ and $30 - 64$, or $N_{\text{side}} = 64$, for $30 - 100$ multipole range and the analysis was performed on these downgraded maps. We removed the dipole and monopole from CMB intensity maps and calculated the quantities $\sum_l C_{l,l+1}^{TT}$ and $\sum_l l(l+1)C_l^{TT}$ over the aforementioned multipole ranges.

Map	S_H^{TT} in 10^{-2} mK^2	A	(l, b)	P-value
Commander	2.55 ± 0.68	0.082 ± 0.018	$(232^\circ \pm 18^\circ, -14^\circ \pm 18^\circ)$	0.20%
SMICA(inp.)	2.39 ± 0.70	0.069 ± 0.013	$(236^\circ \pm 27^\circ, -11^\circ \pm 20^\circ)$	0.70%
SMICA(filled)	2.44 ± 0.71	0.078 ± 0.019	$(242^\circ \pm 16^\circ, -17^\circ \pm 20^\circ)$	0.50%

TABLE I. The maximum TT Mode S_H values along with the dipole modulation parameter A , the preferred direction of maximization and the P-value.

We also used another method to analyze the SMICA maps. In this case the SMICA I maps were first masked with their respective masks. The pixels which were masked were filled with data from I simulated maps generated using lensed scalar C_l values generated with the CAMB Boltzmann solver [24] for the Planck 2015 parameters [25], and the Synfast program from the HEALPix package. The masked and filled I maps have $N_{\text{side}} = 2048$, same as that of the original maps. These maps were smoothed with a FWHM equal to 3 times the pixel size of the low resolution map with $N_{\text{side}} = 256$ before downgrading the map to remove the discontinuities at the mask boundary. The smoothed maps are then degraded to $N_{\text{side}} = 256$ followed by a further degradation to $N_{\text{side}} = 32$ or $N_{\text{side}} = 64$, depending on the multipole range, for final analysis. We generated 100 such filled maps and the individual results were found to depend on the random realization used to fill the masked portions of the sky. The results presented here are the mean values for the statistic S_H^{TT} and direction for which it maximizes. The SMICA I maps masked and reconstructed using these two procedures, i.e. inpainting and random filling, are shown in Fig. 1.

We have fitted the TT mode values of S_H in order to extract the value of the dipole modulation amplitude A of Eq. (I.2). We simulated 100 isotropic CMB maps using Planck 2015 parameters with $N_{\text{side}} = 512$ ($N_{\text{side}} = 1024$ for SMICA filled analysis). These maps were rotated to have the z axis pointing along the direction of maximum statistic and they were modulated using Eq. (I.1). The modulated maps were downgraded to $N_{\text{side}} = 32$. Each of the downgraded simulated maps were fitted for the value of A that would give the value of S_H closest to the one observed in the data along the direction along which it maximizes in the Planck 2015 CMB maps. We averaged over 100 best fit values of A obtained by this method giving the modulation amplitude for the results given in Table I.

To estimate the error in S_H^{TT} we generated 1000 maps at $N_{\text{side}} = 512$ ($N_{\text{side}} = 1024$ for SMICA filled analysis) and modulated the maps with the best-fit value of A along the direction of maxi-

l Range	S_H^{TT} in 10^{-2} mK^2	A	(l, b)	P-value	R
2-64	2.55 ± 0.68	0.082 ± 0.018	$(232^\circ \pm 18^\circ, -14^\circ \pm 18^\circ)$	0.20%	0.065
30-64	1.00 ± 0.43	0.052 ± 0.019	$(194^\circ \pm 25^\circ, -4^\circ \pm 24^\circ)$	66.6%	0.040
30-100	0.91 ± 0.72	0.018 ± 0.011	$(277^\circ \pm 81^\circ, 4^\circ \pm 30^\circ)$	83.0%	0.013

TABLE II. TT mode S_H results for Planck Commander 2015 maps in different multipole ranges.

imum statistic using relation (I.2). The modulated CMB maps were downgraded to $N_{\text{side}} = 32$ or $N_{\text{side}} = 64$ depending on the multipole range under consideration and S_H^{TT} was calculated along the direction of modulation. The standard deviation of the 1000 simulated maps gives the error in S_H^{TT} . For the masked and filled SMICA maps, the process of filling the masked region of the SMICA maps with isotropic data is expected to introduce bias in the obtained results for S_H . This bias correction is relatively small [22] and we ignore it in our analysis. It is expected to enhance the signal by about 8%.

The error estimation in the preferred direction was performed by simulating 50 isotropic temperature maps. We modulated these maps with the best-fit value of A along the observed direction in the data. The direction along which the statistic S_H^{TT} maximises in the maps was found and the standard deviation of the coordinates gave corresponding errors.

Finally to test the significance of our results we simulate 2000 isotropic CMB maps for 2 – 64 multipole range and 500 maps for the other multipole ranges, with Planck 2015 parameters and search for the direction along which the statistic maximizes. The values of S_H obtained by this process is used to obtain probability distribution of the statistic S_H for the isotropic hypothesis. The histogram is given in Fig. 2. P-values for individual results were obtained as the percentage of simulation results that equal or exceed the observed result for the statistic.

B. Planck 2015 polarization data analysis

For the case of polarization, as explained above, we are unable to perform a detailed analysis of dipole modulation. Here we confine ourselves to simply making an estimate of the statistic S_H^{EE} and the corresponding preferred direction using the Commander map. Since the low l multipoles are not expected to be reliable we confine our study to the multipole ranges 40 – 100, 40 – 125, 50 – 100 and 50 – 125. Furthermore we use the dipole modulation model for polarization in order

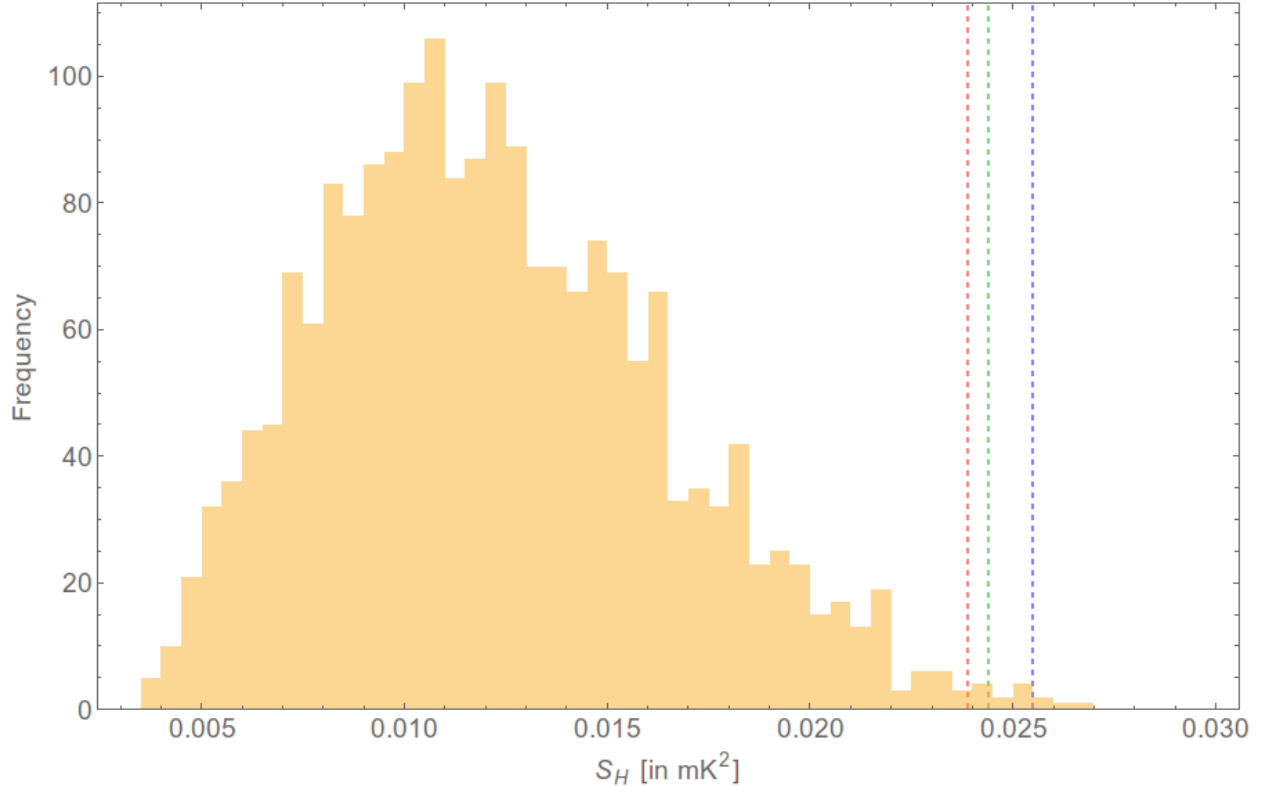


FIG. 2. Histogram of TT S_H values obtained by using isotropic Λ CDM simulations. The observed S_H values are indicated by dashed lines. The results obtained by using the Commander map (blue line), SMICA inpainted (red line) and SMICA filled map (green line) are shown.

to generate simulated maps which display polarization power anisotropy and to determine the distributions of the corresponding statistic S_H for the E mode polarization. The main purpose of this study is to illustrate the utility of this model.

V. RESULTS

In this section we first present the results for the temperature analysis and later those of polarization.

A. Temperature

The TT mode results for multipole range $2 \leq l \leq 64$ are summarized in Table I. As stated in the previous section the dipole modulation in the CMB temperature signal is present in lower

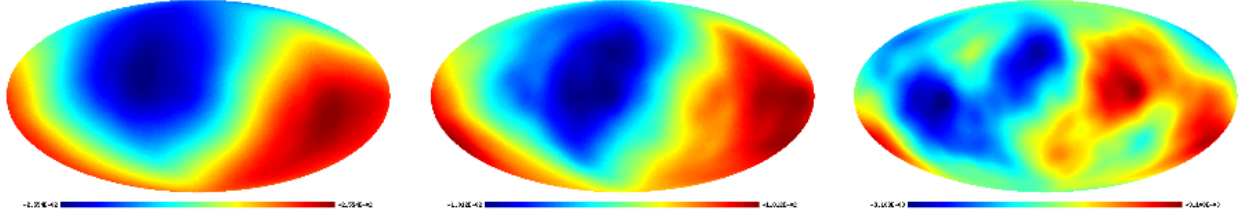


FIG. 3. From the left S_H^{TT} sky maps for Commander data in multipole ranges 2 – 64, 30 – 64 and 30 – 100.

multipoles up to $l = 64$. Our primary TT mode results are for this multipole range. We can compare our results with [22] to look for changes between the Planck 2013 and Planck 2015 data. The results for SMICA filled maps for Planck 2013 data are: $S_H^{TT} = (2.1 \pm 0.5) \times 10^{-2} \text{mK}^2$, a bias corrected value of $(2.3 \pm 0.6) \times 10^{-2} \text{mK}^2$, along $(229^\circ, -16^\circ)$ with $A = 0.074 \pm 0.019$. Comparing the 2013 and 2015 SMICA filled map results we notice agreement in both the values of S_H^{TT} and direction of maximization, while the value of A is also comparable within the error limits. The results for SMICA inpainted map for Planck 2013 data are: $S_H^{TT} = (2.7 \pm 0.7) \times 10^{-2} \text{mK}^2$, along $(232^\circ, -12^\circ)$. For SMICA inpainted maps too, we find good agreement with previous results. We also note that the 2015 results have smaller P-values when compared with isotropic ΛCDM simulations generated using 2015 Planck parameters. We can compare our results with Planck Collaboration's analysis of dipole modulation [26]. Planck 2015 best fit values of modulation amplitude A is $0.063_{-0.013}^{+0.025}$ for Commander maps and $0.062_{-0.013}^{+0.026}$ for SMICA map. The direction of modulation is $(213^\circ, -26^\circ) \pm 28^\circ$ for both SMICA and Commander maps. Both the modulation amplitude and the direction agree with our results within the quoted errors. Our results are also consistent with those obtained in [27].

It has been found by an earlier analysis that the hemispherical anisotropy effect rapidly dies out when the lower multipoles are excluded or when summed to higher multipoles [26, 28–30]. In order to study the multipole dependence we also investigate the effect in the multipole ranges 30 – 64 and 30 – 100. The S_H^{TT} obtained in 30-64 for Commander map is contained in Table II. In this case we do not find a significant signal of $l, l+1$ correlation. The temperature map S_H is very much in agreement with expectations from isotropic theory. We also notice that the S_H^{TT} maximizes along directions which change from one range to another. This can also be seen from Fig. 3. These maps show S_H^{TT} for different directions in ranges 2-64, 30-64 and 30-100. It can be seen that left to right the dipole pattern becomes less distinct.

The SMICA inpainted TT mode results are as follows:

- In the range 30-64, S_H^{TT} maximizes at $(1.24 \pm 0.43) \times 10^{-2} \text{mK}^2$ along $(191^\circ \pm 27^\circ, -4^\circ \pm 28^\circ)$ with a P-value of 45% and $A = 0.059 \pm 0.019$.
- For 30-100 range, S_H^{TT} maximizes at $(1.45 \pm 0.71) \times 10^{-2} \text{mK}^2$ along $(207^\circ \pm 38^\circ, -18^\circ \pm 27^\circ)$ with a P-value of 41.2% and $A = 0.027 \pm 0.013$.

The SMICA filled map temperature results are:

- In 30-64 range, S_H^{TT} maximizes at $(1.00 \pm 0.43) \times 10^{-2} \text{mK}^2$ along $(228^\circ \pm 28^\circ, -9^\circ \pm 27^\circ)$ with a P-value of 66% and $A = 0.055 \pm 0.021$.
- The 30-100 range S_H^{TT} maximizes at $(1.64 \pm 0.77) \times 10^{-2} \text{mK}^2$ along $(238^\circ \pm 34^\circ, -11^\circ \pm 28^\circ)$ with a P-value of 27% and $A = 0.031 \pm 0.014$.

Both SMICA inpainted and filled maps results show similar patterns as Commander map results.

B. Polarization

In this section we present our results for polarization. As explained above, we do not make an attempt to compute either the errors or the significance of this effect due to uncertainties in the noise simulation in polarization. However we do present the results of a simulation in order to illustrate the utility of the polarization dipole modulation model, Eq. III.2.

In Table III we give the results for S_H^{EE} , the preferred direction and the ratio R for the E mode polarization. The result for the case of the multipole range 40 – 100 is mildly interesting. This is because the preferred direction aligns closely with the CMBR dipole. A preferred direction similar to the one obtained in the range 40 – 100 has been seen in many other studies [31, 32], including the radio polarization dipole axis [33], the CMB quadrupole – octopole alignment axis [34], the NVSS dipole [35–38], the radio polarization flux dipole axis [39] as well as the optical polarizations from distant quasars [31, 40–42]. It is possible that the present signal in E mode polarization in this range arises from some residual contamination of the low l noise systematic bias. Alternatively it may be a signal of some astrophysical or cosmological effect. This may be settled by future refinements in data.

For the higher multipole ranges the preferred direction starts to deviate. For example, in the multipole range 40 – 125, 50 – 100, 50 – 125 it lies closer to the galactic plane. This might be

l Range	S_H^{EE} in 10^{-6} mK^2	(l, b)	R
40-100	6.6	$(260^\circ, 44^\circ)$	0.031
40-125	9.4	$(291^\circ, 14^\circ)$	0.023
50-100	6.6	$(286^\circ, 15^\circ)$	0.033
50-125	9.5	$(291^\circ, 14^\circ)$	0.025

TABLE III. EE mode S_H results for Planck Commander 2015 maps in different multipole ranges.

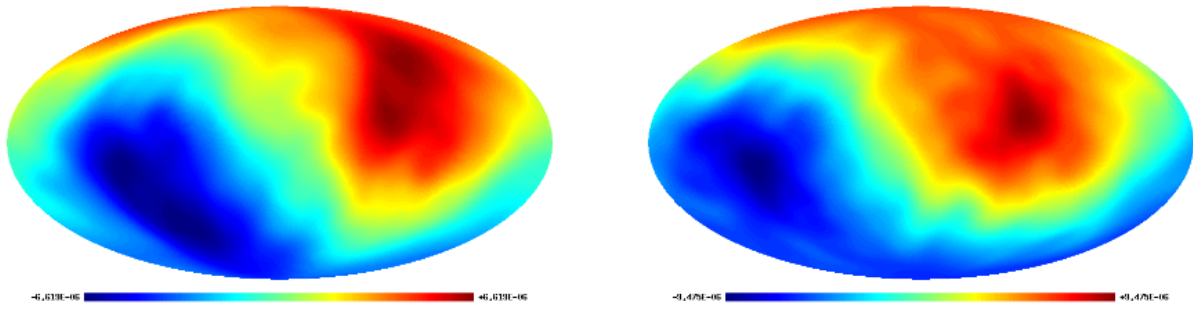


FIG. 4. The S_H^{EE} sky maps for Commander data in multipole ranges 40 – 100 (left) and 40 – 125 (right).

an indication that it is moving closer to the axis obtained in the case of temperature. Alternatively, since it lies very close to the galactic plane, the signal in this range might be dominated by foregrounds. The plots of S_H^{EE} for the multipole range 40 – 100 and 40 – 125 are shown in Fig. 4.

We next generate 1000 simulated Q and U mode polarization maps which include dipole modulation with parameter $A_1 = 0.05$ for the multipole range 40 – 100. We compute the statistics S_H^{EE} for these simulated maps. The resulting distribution of this statistics is shown in Fig. 5. We find that the distribution is close to normal. The parameter chosen is not too far from what might be required to fit the E mode results given in Table III.

VI. CONCLUSIONS

This work has updated the previous results for dipole modulation in CMB temperature field. We find that the dipole modulation of the temperature field, observed in WMAP data and Planck 2013 data is also present in Planck 2015 data. We have computed the quantity S_H^{TT} and the results are found to be in agreement with the values obtained from the previous data [22]. Our result for

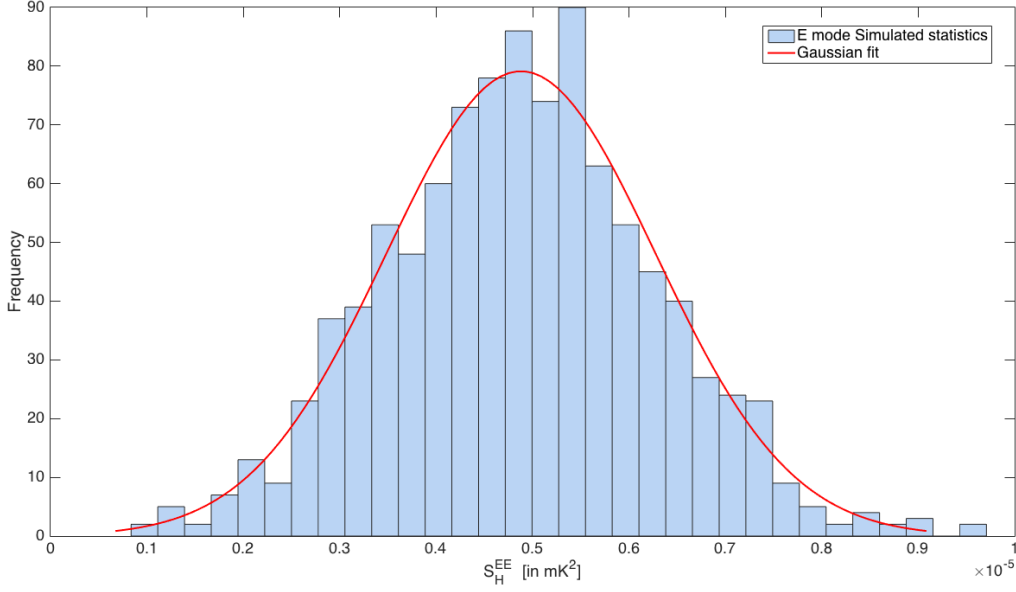


FIG. 5. The S_H^{EE} histogram for the simulated dipole modulated E mode polarization maps with the parameter $A_1 = 0.05$.

modulation parameter A and modulation direction are compatible with Planck 2015 results [26].

We have presented a preliminary analysis of the dipole modulation in the CMBR polarization. In this case we confine our analysis only to the multipole values $l > 40$ since the lower l values are not expected to be reliable. The detector noise is expected to make considerable contribution in this case. Since this information is not available to us, we do not attempt to compute the significance of the signal or the associated error in extracted parameters. In any case our preliminary investigation reveals some interesting results about the direction of the signal. We find that for the range of multipoles $40 - 100$ the preferred direction is close to the CMBR dipole and for a slightly higher range $50 - 100$ or $40 - 125$, the direction shifts closer to the galactic plane. The direction found for the lower range of multipoles is somewhat interesting since a similar direction has been found in several other data sets [31–39].

For the case of polarization we also propose a dipole modulation model, Eq. III.2. This is a useful model which generalizes the temperature dipole modulation [9–12], Eq. I.1, to the case of polarization. We find that this model leads to correlations between l and $l + 1$ multipoles of the polarization field. We determine the form of these correlations for the case of EE , BB and TE fields. We show the utility of this model by creating simulated polarization maps with non-

zero values of the dipole modulation parameter, A_1 . We find that distribution of the resulting statistic for the case of E model polarization is well described by a Gaussian. We expect that this dipole modulation model and our proposed analysis procedure may be very useful in the study of anisotropy which might exist in the CMBR polarized field.

VII. APPENDIX

In this Appendix we derive the mathematical results required in proving the results in section III B. Let $f(n, p)$ be defined as

$$f(n, p) = \sum_{r=0}^n r^p (-1)^r \binom{n}{r} \quad (\text{VII.1})$$

where $n, p \geq 0$. This function satisfies the recurrence relation

$$f(n, p+1) = \begin{cases} (-n) \sum_{q=0}^p f(n-1, q) \binom{p}{q} & n \neq 0 \\ 0 & n = 0 \end{cases}. \quad (\text{VII.2})$$

Proof: The result for $n = 0$ can be verified by direct substitution. For $n > 0$, we can write $f(n, p+1)$ as

$$f(n, p+1) = n \sum_{r=0}^n (-1)^r r^p \frac{(n-1)!}{(n-r)!(r-1)!}.$$

On the right hand side the term corresponding to $r = 0$ is zero due to the factor $(r-1)!$ in the denominator. Hence we can start the sum from $r = 1$. Setting $r-1 = t$, we obtain

$$f(n, p+1) = -n \sum_{t=0}^{n-1} (-1)^t (1+t)^p \frac{(n-1)!}{(n-t-1)!t!} = -n \sum_{q=0}^p \binom{p}{q} \sum_{t=0}^{n-1} (-1)^t \binom{n-1}{t} t^q,$$

where we have used the binomial theorem. Furthermore

$$f(n-1, q) = \sum_{t=0}^{n-1} (-1)^t \binom{n-1}{t} t^q,$$

and hence

$$f(n, p+1) = -n \sum_{q=0}^p f(n-1, q) \binom{p}{q}.$$

This proves the result in Eq. VII.2 for $n \neq 0$.

The function $f(n, p)$ defined in Eq. VII.1 is given by

$$f(n, p) = \begin{cases} 0 & p < n, n \neq 0 \\ (-1)^n n! & p = n, n \geq 0 \\ \frac{n(n+1)}{2} (-1)^n n! & p = n+1, n \geq 0 \end{cases} \quad (\text{VII.3})$$

Proof: The first part can be proven by using the Corollary 2 of [43] with $x = 0$ and $p = n - j$. The result follows since $p < n$ when $1 \leq j \leq n$. Furthermore the second part can be obtained by using Theorem 1 of [43] with $x = 0$.

Finally we consider the last part. By using Eq. VII.2 we find that for $n = 0$, $p = n + 1$, $f(0, p) = 0$, which agrees with the result given in Eq. VII.3. We next consider $n > 0$. By using Eq. VII.2 we obtain

$$f(n, n+1) = -n \sum_{q=0}^n f(n-1, q) \binom{n}{q} = -n \left[f(n-1, n-1) \binom{n}{n-1} + f(n-1, n) \right].$$

That is, the only nonvanishing terms in this sum are obtained by setting $q = n - 1$ and $q = n$. Using the second case of Eq. VII.3 this can be further simplified in the form of the following recurrence relation:

$$P(n) = -n [-(-1)^n n! + P(n-1)], \quad (\text{VII.4})$$

where $P(n) = f(n, n+1)$. We next proceed by induction. For $n = 1$, by using VII.1 we obtain

$$P(1) = f(1, 2) = -1,$$

which agrees with the result given in Eq. VII.3. We next assume that this result is true for $n = k$, i.e.,

$$P(k) = \frac{k(k+1)}{2} (-1)^k k!$$

and show that it is also true for $P(k+1)$. By using recurrence relation VII.4 we obtain

$$P(k+1) = -(k+1) \left[-(-1)^{k+1} (k+1)! + \frac{k(k+1)}{2} (-1)^k k! \right] = \frac{(k+1)(k+2)}{2} (-1)^{k+1} (k+1)!$$

which agrees with Eq. VII.3. Hence the third part is also proven by induction.

ACKNOWLEDGMENTS

Rahul Kothari sincerely acknowledges CSIR, New Delhi for the award of fellowship during the work. Some of the results in this paper have been derived using HealPix package [44]. We used standard Boltzmann solver CAMB (<http://camb.info/readme.html>) for our theoretical calculations and acknowledge the use of PLANCK data available from NASA LAMBDA site (<http://lambda.gsfc.nasa.gov>). We are very grateful to Anthony Banday and Yashar Akrami for

explaining the limitations of the PLANCK polarization data. Finally we thank J. L. Starck for a useful correspondence.

-
- [1] H. K. Eriksen, F. K. Hansen, A. J. Banday, K. M. Górski, and P. B. Lilje, *Astrophys.J.* **605**, 14 (Apr. 2004), [astro-ph/0307507](#)
 - [2] H. K. Eriksen, A. J. Banday, K. M. Górski, F. K. Hansen, and P. B. Lilje, *Astrophys.J.* **660**, L81 (May 2007), [astro-ph/0701089](#)
 - [3] A. L. Erickcek, M. Kamionkowski, and S. M. Carroll, *Phys. Rev. D* **78**, 123520 (Dec. 2008), [arXiv:0806.0377](#)
 - [4] F. K. Hansen, A. J. Banday, K. M. Górski, H. K. Eriksen, and P. B. Lilje, *Astrophys.J.* **704**, 1448 (Oct. 2009), [arXiv:0812.3795](#)
 - [5] J. Hoftuft, H. K. Eriksen, A. J. Banday, K. M. Górski, F. K. Hansen, and P. B. Lilje, *Astrophys.J.* **699**, 985 (Jul. 2009), [arXiv:0903.1229](#) [[astro-ph.CO](#)]
 - [6] F. Paci, A. Gruppuso, F. Finelli, A. De Rosa, N. Mandolesi, and P. Natoli, *MNRAS* **434**, 3071 (Oct. 2013), [arXiv:1301.5195](#)
 - [7] Planck Collaboration, P. A. R. Ade, N. Aghanim, C. Armitage-Caplan, M. Arnaud, M. Ashdown, F. Atrio-Barandela, J. Aumont, C. Baccigalupi, A. J. Banday, and et al., *Astron.Astrophys.* **571**, A23 (Nov. 2014), [arXiv:1303.5083](#)
 - [8] Y. Akrami, Y. Fantaye, A. Shafieloo, H. K. Eriksen, F. K. Hansen, A. J. Banday, and K. M. Górski, *Astrophys.J.* **784**, L42 (Apr. 2014), [arXiv:1402.0870](#)
 - [9] C. Gordon, W. Hu, D. Huterer, and T. Crawford, *Phys. Rev. D* **72**, 103002 (Nov. 2005), [astro-ph/0509301](#)
 - [10] C. Gordon, *Astrophys.J.* **656**, 636 (Feb. 2007), [astro-ph/0607423](#)
 - [11] S. Prunet, J.-P. Uzan, F. Bernardeau, and T. Brunier, *Phys. Rev. D* **71**, 083508 (Apr. 2005), [astro-ph/0406364](#)
 - [12] C. L. Bennett, R. S. Hill, G. Hinshaw, D. Larson, K. M. Smith, J. Dunkley, B. Gold, M. Halpern, N. Jarosik, A. Kogut, E. Komatsu, M. Limon, S. S. Meyer, M. R. Nolte, N. Odegard, L. Page, D. N. Spergel, G. S. Tucker, J. L. Weiland, E. Wollack, and E. L. Wright, *Astrophys.J.Suppl.* **192**, 17 (Feb. 2011), [arXiv:1001.4758](#) [[astro-ph.CO](#)]
 - [13] P. K. Rath and P. Jain, *JCAP* **1312**, 014 (2013), [arXiv:1308.0924](#) [[astro-ph.CO](#)]

- [14] M. Namjoo, A. Abolhasani, H. Assadullahi, S. Baghran, H. Firouzjahi, et al., JCAP **1505**, 015 (2015), arXiv:1411.5312 [astro-ph.CO]
- [15] R. Kothari, S. Ghosh, P. K. Rath, G. Kashyap, and P. Jain(2015), arXiv:1503.08997 [astro-ph.CO]
- [16] M. Zaldarriaga and U. Seljak, Phys.Rev. **D55**, 1830 (1997), arXiv:astro-ph/9609170 [astro-ph]
- [17] M. Kamionkowski, A. Kosowsky, and A. Stebbins, Phys.Rev. **D55**, 7368 (1997), arXiv:astro-ph/9611125 [astro-ph]
- [18] E. T. Newman and R. Penrose, Journal of Mathematical Physics **7**, 863 (1966)
- [19] J. N. Goldberg, A. J. Macfarlane, E. T. Newman, F. Rohrlich, and E. C. G. Sudarshan, Journal of Mathematical Physics **8**, 2155 (Nov. 1967)
- [20] M. Abramowitz and I. A. Stegun, Handbook of Mathematical Functions, New York: Dover, 1972 (1972)
- [21] J. Gallier, Discrete Mathematics, Springer, 2011 (2011)
- [22] P. K. Rath, P. K. Aluri, and P. Jain, Phys.Rev. **D91**, 023515 (2015), arXiv:1403.2567 [astro-ph.CO]
- [23] K. Gorski, E. Hivon, A. Banday, B. Wandelt, F. Hansen, et al., Astrophys.J. **622**, 759 (2005), arXiv:astro-ph/0409513 [astro-ph]
- [24] A. Lewis, A. Challinor, and A. Lasenby, Astrophys.J. **538**, 473 (2000), arXiv:astro-ph/9911177 [astro-ph]
- [25] P. Ade et al. (Planck)(2015), arXiv:1502.01589 [astro-ph.CO]
- [26] P. Ade et al. (Planck)(2015), arXiv:1506.07135 [astro-ph.CO]
- [27] S. Aiola, B. Wang, A. Kosowsky, T. Kahniashvili, and H. Firouzjahi, ArXiv e-prints(Jun. 2015), arXiv:1506.04405
- [28] E. P. Donoghue and J. F. Donoghue, Phys. Rev. D **71**, 043002 (Feb. 2005), astro-ph/0411237
- [29] D. Hanson and A. Lewis, Phys. Rev. D **80**, 063004 (Sep. 2009), arXiv:0908.0963 [astro-ph.CO]
- [30] M. Quartin and A. Notari, JCAP **1**, 008 (Jan. 2015), arXiv:1408.5792
- [31] J. P. Ralston and P. Jain, IJMPD **13**, 1857 (2004), arXiv:astro-ph/0311430 [astro-ph]
- [32] D. J. Schwarz, G. D. Starkman, D. Huterer, and C. J. Copi, Phys. Rev. Lett. **93**, 221301 (Nov 2004)
- [33] P. Jain and J. P. Ralston, Mod. Phys. Lett. A **14**, 417 (1999)
- [34] A. de Oliveira-Costa, M. Tegmark, M. Zaldarriaga, and A. Hamilton, Phys.Rev. **D69**, 063516 (2004), arXiv:astro-ph/0307282 [astro-ph]
- [35] A. K. Singal, ApJL **742**, L23 (2011), arXiv:1110.6260 [astro-ph.CO]
- [36] C. Gibelyou and D. Huterer, MNRAS **427**, 1994 (2012), arXiv:1205.6476 [astro-ph.CO]

- [37] M. Rubart and D. J. Schwarz, *A & A* **555**, A117 (2013), arXiv:1301.5559 [astro-ph.CO]
- [38] R. Kothari, A. Naskar, P. Tiwari, S. Nadkarni-Ghosh, and P. Jain, *Astroparticle Physics* **61**, 1 (Feb. 2015), arXiv:1307.1947 [astro-ph.CO]
- [39] P. Tiwari and P. Jain, *MNRAS* **447**, 2658 (Mar. 2015), arXiv:1308.3970
- [40] D. Hutsemékers, *Astron.Astrophys.* **332**, 410 (1998)
- [41] D. Hutsemékers and H. Lamy, *Astron.Astrophys.* **367**, 381 (2001)
- [42] P. Jain, G. Narain, and S. Sarala, *MNRAS* **347**, 394 (2004)
- [43] S. Ruiz, *The Mathematical Gazette* **80**, 489 (1996)
- [44] K. Gořski, E. Hivon, A. Banday, B. Wandelt, F. Hansen, et al., *ApJ* **622**, 759 (2005), arXiv:astro-ph/0409513 [astro-ph]CITATION = ASTRO-PH/0409513